Proceedings of the 9th International Conference on Aluminium Alloys (2004)
Edited by J.F. Nie, A.J. Morton and B.C. Muddle

Simulation of Concurrent Precipitation Effect on Recrystallisation Kinetics in AA3103

A. Miroux[1], E. Anselmino[1], S. van der Zwaag[2]

[1] Netherlands Institute for Metals Research, Rotterdamseweg 137, 2628 AL Delft, The Netherlands
[2] Faculty Aerospace Engineering, Kluyverweg 1, 2629 HS Delft, The Netherlands

Keywords: recrystallization, precipitation, recovery, modeling, aluminium alloy

Abstract

A recrystallisation model including recovery is used to study particle pinning effects on recrystallisation kinetics. Results show that both pinning of grain and subgrain boundaries have to be considered. As they have opposite influences on the recrystallisation kinetics the total effect can only be predicted by using a model. The analysis shows how to simply estimate the effect of particle pinning and the potential relevance of concurrent precipitation. The way of quantifying particles is also shown to be significant.

1. Introduction

Developing efficient models for predicting recrystallisation kinetics after hot or cold deformation has been an issue for many years in the metal industry. Among important factors that interact with recrystallisation and then control the recrystallisation kinetics precipitates and second phase particles usually play a major role. Particles are generally considered for their pinning effect on moving grain boundaries of recrystallising grains through the so-called Zener pinning mechanism. However particles also interact with subgrain boundaries and then with recovery.

The aim of this study is to show how it is possible to use the classical recrystallisation theory and commonly accepted equations to quantify the simultaneous influence of precipitates on recovery and recrystallisation and to discuss the potential relevance of concurrent precipitation during recrystallisation. In order to present a clear analysis focused on pinning effects on growing grains, the influence of solutes and the effect of particles on nucleation of recrystallised grains have been neglected. As an example, simulations have been performed using data from the back annealing of AA3103.

2. Model

The driving force for recrystallisation is the consumption of the energy stored in the deformed matrix in front of the moving grain boundary. As aluminum alloys usually form a cell or subgrain substructure during deformation, the stored energy is assumed to be the energy of the subgrain boundaries. Subgrains are described by their mean equivalent radius R_{sg} and mean misorientation θ_{sg}. The surface energy of subboundaries (γ_{sg}) is calculated by the Read-Shockley equation.

The driving pressure for recrystallisation due to an array of equiaxed subgrains is

$$P_D = 1.5\frac{\gamma_{sg}}{R_{sg}}. \quad (1)$$

Recrystallised grains are assumed to be spherical with a radius R and a grain boundary surface energy γ. They grow isotropically with a growth rate given by the classical form

$$\frac{dR}{dt} = M\left(P_D + P_C + P_Z\right). \quad (2)$$

P_c is the retarding pressure due to the curvature of the recrystallised grain boundary

$$P_C = -2\frac{\gamma}{R} \quad (3)$$

and P_z is the Zener pinning force.

Recrystallised grains are assumed to have a high angle grain boundary with the deformed matrix. The boundary motion is thermally activated. The grain boundary mobility (M) is

$$M = M_0 e^{-\frac{Q_{rex}}{R_g T}}. \quad (4)$$

M_0 is the pre-exponential factor and Q_{rex} is the recrystallisation activation energy.

The extended recrystallised fraction ($X_{v\text{-}ex}$) is first calculated ignoring hard impingement between recrystallised grains. The final recrystallisation fraction (X_v) is obtained using the concept of extended volume

$$X_v = 1 - e^{-X_{v-ex}}. \quad (5)$$

Recovery is assumed to take place by subgrain growth. The subgrain grow rate is also in the form

$$\frac{dR_{sg}}{dt} = M_{sg}\left(P_{D-sg} + P_{Z-sg}\right). \quad (6)$$

$P_{z\text{-}sg}$ is the Zener pinning force acting on subboundaries and $P_{d\text{-}sg}$ is the driving pressure for recovery

$$P_{D-sg} = \frac{\gamma_{sg}}{4.R_{sg}}. \quad (7)$$

The subboundary misorientation (θ_{sg}) and then γ_{sg} are assumed to be constant during annealing.

The mobility of the subboundary (M_{sg}) depends on its misorientation and is given by

$$M_{sg} = M\left(1 - e^{-5\left(\frac{\theta_{sg}}{\theta_m}\right)^4}\right) \quad (8)$$

where θ_m is the minimum misorientation of a high angle grain boundary.

Several equations have been proposed for the Zener pinning force [1]. For the current analysis equations proposed by Gladman [2] have been chosen because they are widely used and of clear explanation. They assume spherical grains and particles and incoherent particles. They also ignore the interface tension between particle and grain boundary and do not consider any special shape of the particle – grain boundary interface. During their

growth, recrystallised grains are assumed to see a random distribution of particle and the Zener pinning force is

$$P_Z = -\frac{3}{2}\frac{f\gamma}{r}. \quad (9)$$

Particles are assumed to be located on the subgrain boundaries. Accordingly the Zener pinning force acting on subboundary is

$$P_{Z-sg} = -\frac{1}{2}\frac{f\gamma R_{sg}}{r^2} \quad (10)$$

where f is the volume fraction of particles and r the mean particle radius.

Nucleation is not modeled. A site saturation nucleation is assumed which is generally a good approximation for aluminum alloys. The size of the nuclei (R_{nuc}) is chosen slightly bigger, of a factor α_{nuc}, than the critical size of a grain that neither grows or neither shrinks:

$$R_{nuc} = \alpha_{nuc}\frac{2\gamma}{P_D - P_Z}. \quad (11)$$

3. Input

Simulations are performed for the back annealing of AA3103 after cold rolling. The annealing treatment consists of a slow heating at rate of about 0.7°C/min followed by an isothermal annealing and then cooling.

The cold rolled state of this material before annealing has been characterised by Sjølstad [3]. The mean subgrain sizes are respectively 0.45 μm and 0.71 μm in the normal and rolling direction, which gives an initial equivalent radius of R_{sg} = 0.32 μm. The measured mean subgrain boundary misorientation is θ_{sg} = 4.2°. The calculated subboundary surface energy is then γ_{sg} = 0.206 J/m^2.

The main alloying elements of AA3103 are Mn (1.03 wt.%), Fe (0.49 wt.%) and Si (0.06 wt.%). The material contains two main types of particles: constituent particles and dispersoids. The relevant particles for calculating Zener pinning forces are the dispersoids which size is usually less than 1 μm. Dispersoids have been quantified in detail by Anselmino et al. [4] on the cold rolled and annealed material. The 2 dimensional measured particle size distributions have been recalculated to an equivalent 3 dimensional size distribution using a modified Johnson-Saltykov method [5] (Table 1). Zener pinning forces due to dispersoids of each size class have been calculated and their sum gives the "pinning force from size distribution". Results show that pinning forces calculated from average values is about 1.6 times higher than the one calculated from the size distribution. Ekström et al. [6] reported the same effect and found an overestimation of a factor of 3.

The activation energy for recrystallisation has been determined on this material by Sjølstad [3] and is Q_{rex} = 180 kJ/mol. Using the activation energy and pre-exponential factor determined by Chen [7] for a AA3003 and the compensation effect [8] the pre-exponential factor has been calculated to be M_0 = 1125 m^4/J.s. The minimum misorientation of a high angle grain boundary is chosen to be θ_m = 15°. The surface energy of a high angle grain boundary is γ_m = 0.324 J/m^2. As recrystallised grains are assumed to have a high angle grain boundary $\gamma = \gamma_m$.

Table 1: Dispersoids density, surface or volume fraction and radius in the cold rolled and annealed AA3103. Calculated corresponding Zener pinning forces (P_Z). The equivalent average radius is calculated from the density and surface or volume fraction. The equivalent Zener radius is the particle radius that gives the same pinning force than the one calculated from the particle size distribution.

		Density	Surface or volume fraction	Equivalent average radius	Pinning force from equivalent radius	Pinning force from size distribution	Equivalent Zener radius
		(nb / m^2 or m^3)		(μm)	(MPa)	(MPa)	(μm)
Cold rolled	2D	1.41 10^{11}	0.00282	0.080	0.0172		
Cold rolled	3D	1.60 10^{18}	0.00283	0.075	0.0183	0.0116	0.119
Annealed	2D	1.28 10^{11}	0.00399	0.100	0.0195		
Annealed	3D	1.27 10^{18}	0.00399	0.091	0.0213	0.0128	0.152

Two parameters describing nucleation are necessary: the starting recrystallisation temperature and the nucleus density. In the current analysis, these values have been arbitrary chosen. Recrystallisation is assumed to start at 315°C and a recrystallised grain size of 50 μm is chosen which gives 1.5 10^{13} nuclei/m^3. The factor for the nucleus size is chosen to equal to α_{nuc} = 1.09.

4. Recrystallisation Kinetics Analysis

Table 1 shows that dispersoids grow during back annealing (size and volume fraction increase). There is also some coarsening as the dispersoid density decreases and the mean size increases. Figure 1 present simulations using constant dispersoid sizes and volume fractions. From the results, it is seen that the increase of the Zener pinning force between cold rolled and annealed states is too small to have a visible effect on the recrystallisation kinetics. Even if coarsening is neglected (i.e. dispersoid density kept constant between cold rolled and annealed states) the calculated recrystallisation kinetics remain very close. This small effect of particle pinning can be predicted by comparing P_z on table 1 to the initial driving pressure ($P_D(t = 0)$ = 0.97 MPa) or even to the driving pressure at the onset of recrystallisation ($P_D(t$ = 428 min) = 0.4 MPa)[1]. Even when considering possible variations of initial subgrain size and misorientation P_Z is significantly lower than P_D. Taking into account concurrent precipitation to model the growth of recrystallised grain is not necessary for the current example and the assumption of a constant dispersoid population is valid.

On the other hand, figure 1 shows that calculating Zener pinning forces from the dispersoids size distribution ("r-Zener") leads to a slower recrystallisation kinetics than those obtained with pinning forces calculated from equivalent average dispersoid radii ('r-av"). More surprising is the speed up of the recrystallisation kinetics with increasing the Zener pinning force. To understand this effect simulations have been done with pinning forces varying in a larger range.

[1] The net driving pressure for the growth of a nucleus is $P_{tot} = (P_D - P_Z)(1-1/\alpha_{nuc})$. P_Z has to be compare to P_D only.

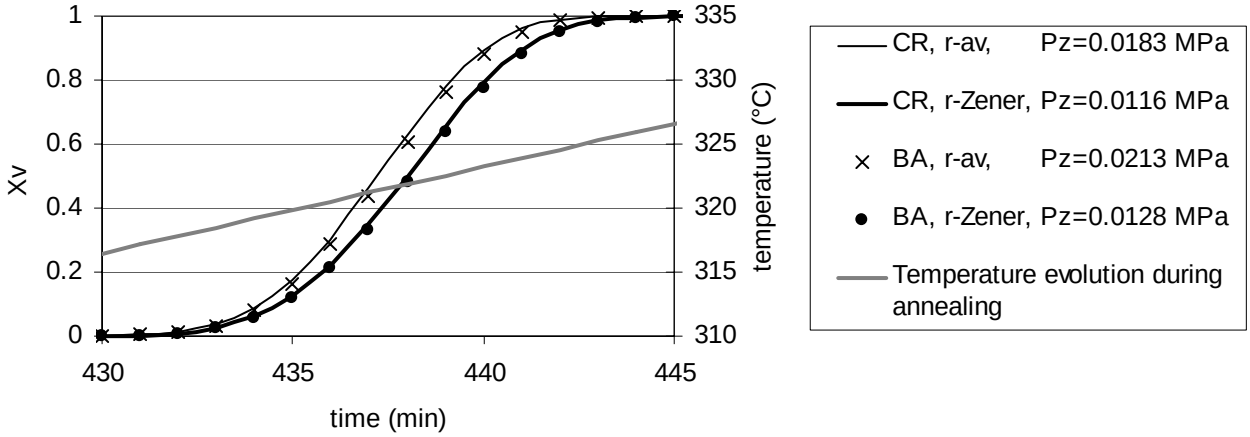

Figure 1: Recrystallisation kinetics for 4 dispersoids populations. CR and BA are simulations using dispersoid radius and volume fraction measured respectively in the cold rolled and back-annealed materials. r-av and r-Zener indicate the use of equivalent average radius or equivalent Zener radius.

First, simulations have been done assuming “no recovery” (i.e. keeping maximum driving force) or with “recovery but without subboundary pinning” (i.e. maximum recovery rate or minimum driving force) for various values of the Zener pinning force. Results on figure 2 show that for both cases recrystallisation slows down as expected when the pinning force increases. For the same P_z, kinetics obtained without recovery are logically faster than those with recovery but without subboundary pinning.

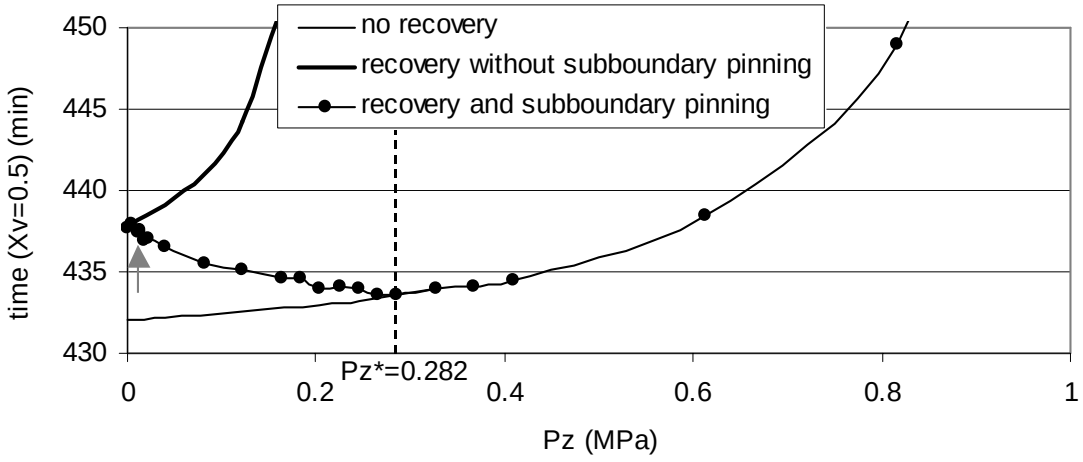

Figure 2: Time for 50% recrystallisation as a function of the Zener pinning force.

If recovery and subboundary pinning are taken into account, both grain boundaries and subboundaries interact with particles resulting in the more complex behaviour seen on figure 2 for the curve “recovery and subboundary pinning”. The curves “recovery without subboundary pinning” and “recovery and subboundary pinning” start normally at the same point for P_z = 0 MPa. For $P_z > P_z^*$, pinning forces on subboundaries are high enough to prevent any subgrain growth from the beginning of annealing. On this part the curve “no recovery” and “recovery and subboundary pinning” overlap. Between 0 and P_z^*, particles are more efficient to pin subboundaries and to maintain a high driving force for recrystallisation than to retard grain boundary motion; an increase in P_z is counterbalanced by a higher driving force (P_D) due to a slower recovery rate. This effect results to faster

recrystallisation kinetics with increasing P_z. P_z* can be calculated from the radius and volume fraction of particles that give $P_{Z\text{-}sg} = P_{D\text{-}sg}$ at t = 0 s.

Simulations presented on figure 1 correspond to Zener pinning forces indicated by an arrow in figure 2. This corresponds obviously to the case $P_z < P_z$* and explains why the recrystallisation kinetics where slower for the cases “r-Zener” than for the cases “r-av”.

In the above analysis the influence of particles and precipitation on nucleation of recrystallised grains has been neglected. However it is expected that an increase of pinning forces will delay nucleation and decrease the nuclei density, both effect leading to a slower recrystallisation kinetics and to a higher time(Xv = 0.5). This will probably have a significant effect on the curves in figure 2 [7-9-10] but a quantitative analysis of precipitation interaction with nucleation is out of the scope of the present study.

5. Conclusion

Particle pinning influence on the growth of recrystallising grains has been analysed with the means of a simple model. Results show that particle pinning should not be regarding only for its retardation effect on growing recrystallised grains. The influence of particles on recovery kinetics is of first order and can produce subtle effects as an increase of recrystallisation kinetics with increasing pinning forces. To quantify the importance of particle pinning for a specific alloy and process, Zener pinning forces have to be first compared with the driving forces for recovery and recrystallisation. Using average particle volume fractions and radii can overestimate the calculated pinning forces and calculation from a particle size distribution is more accurate. Calculation of graphs as in figure 2 allows a finer quantitative analysis on how particle pinning can affect recrystallisation. It is also useful to estimate which variation of Zener pinning due to concurrent precipitation can influence the recrystallisation kinetics. Only when P_z is much larger than P_z* or when P_z varies within a large range, a significant effect is expected.

References

[1] P.A. Manohar, M. Ferry and T. Chandra, ISIJ inter., 38, 9, 913-924,1998.
[2] T. Gladman, Scripta Metall. & Mater., 27, 1569-73, 1992.
[3] K. Sjølstad, Ph.D. Thesis, NTNU, Thondheim, Norway, 2003.
[4] E. Anselmino, A. Miroux and S van der Zwaag, submitted for publication in Materials Characterisation.
[5] E. Anselmino, A. Miroux and S van der Zwaag, G.G.E. Seward, N.C.A. Seaton, D.J. Prior, submitted for publication in proc. of ICAA9 conf.
[6] H.-E. Ekström, J. Hagström and B. Hutchinson, Proc. 4th Inter. Conf. on Recrystallization and Related Phenomena, ed. T. Sakai and H. G. Suzuki, The Japan Institute of Metals, 1999.
[7] S. P. Chen, Ph.D. Thesis, Technical University Delft, Delft, The Netherlands, 2003.
[8] Y. Huang and F. J. Humphreys, Recrystallization and Grain Growth Proc. of the 1st Joint Inter. Conf., Eds. G. Gottstein and D.A. Molodov, Springer-Verlag, 2001.
[9] F. J. Humphreys, Acta Mater., 45, 12, 5031-5039, 1997.
[10] K. Marthinsen, O. Daaland, T. Furu and E. Nes, Metall. & Mater. Trans. A, 34A, 2705-2715, 2003.